Application of design of experiments (DoE) in evaluating crushing-screening performance for aggregates production

(article starts on next page)

Minerals Engineering 209 (2024) 108616

Contents lists available at ScienceDirect

Minerals Engineering

journal homepage: www.elsevier.com/locate/mineng

Application of design of experiments (DoE) in evaluating crushing-screening performance for aggregates production

Kanishk Bhadani [a,*], Gauti Asbjörnsson [a], Kristoffer Hofling [b], Erik Hulthén [a], Magnus Evertsson [a]

[a] *Department of Industrial and Materials Science, Chalmers University of Technology, Gothenburg, Sweden*
[b] *NCC Industry AB, Division Stone Materials, Uddevalla, Sweden*

ARTICLE INFO

Keywords:
Crushing
Screening
Design of experiments
Response modelling
Comminution
Aggregate production
Digital experiments

ABSTRACT

The configuration and the interaction between the crushers and screens enable aggregate producers to produce products that are in accordance with the applicable product certification. However, the performance of the system is seldom optimized for the given conditions and market demand. This paper aims to describe the experimental work and the results of quantifying the crusher and screen performance by applying the design of experiments (DoE) in a full-scale tertiary crushing process of an aggregate production plant with both standard belt-cut sampling as well with continuous processes monitoring. The results show the application of a simplified modelling approach using the design of experiments for the evaluation of crusher performance and circuit performance using experimental data. The research output is able to demonstrate that there exists an interaction effect between the crusher closed side setting and eccentric speed that previously has not been identified with traditional methods. The quantification of interaction between crusher and screen individual performance to the process performance has been demonstrated with both belt-cut samples and continuous process monitoring. Using a DoE, digital experiments can be planned for mapping and quantifying the performance of aggregate production.

1. Introduction

In the production of aggregates, the size reduction and classification of the stream are necessary to go from blasted material to saleable products. This is carried out through several stages, often involving jaw and cone crushers for size reduction as well as the usage of inclined vibrating screens for separating the streams based on particle sizes. The performance of each unit in the process and their interaction effect contribute to the total efficiency of the entire process. For each unit, the performance depends on the geometric design, condition and configuration of each operational unit, the plant́s configuration, the design of the control and physical properties of the incoming feed (Asbjörnsson, 2015).

The individual crusher performance has been quantified in different manners. The performance is usually defined by capacity and size reduction i.e., the difference between the 80 % passing size in the feed (F80) and the 80 % passing size in the product (P80). However, additional factors such as yield (Bearman and Briggs, 1998; Evertsson, 2000), particle shape (Bengtsson, 2009), total reduction (Lindqvist and Li, 2021) and even liberation (Guldris Leon et al., 2020) have been applied to evaluate the performance of compressive crushing. In addition to the product-related outputs, internal variables, such as pressure and power, can indicate how well the crusher is operated and fed (Asbjörnsson et al., 2020). Different design and operational variables of a cone crusher have been studied individually by multiple researchers. This includes closed-side setting (*CSS*) (Evertsson, 2000), eccentric throw (Evertsson, 2000), eccentric speed (*ES*) (Hulthén, 2010; Jacobson et al., 2010), filling level (Jacobson et al., 2010), chamber design (Lee, 2012), wear (Lindqvist, 2005), feed composition (Fuerstenau and Venkataraman, 1988), feeding arrangement (Gröndahl et al., 2018) and size of the crusher. All proved to significantly impact the crusher and corresponding process performance.

In a similar aspect, the vibratory screen screening performance is measured in different aspects such as efficiency, capacity, and quality (Bengtsson, 2009; Wills and Finch, 2015). For a vibratory screen, various research has been conducted to study the effect of internal operational and design variables on the performance such as passage rate probability and stratification (Soldinger, 2002); wear and panel design (Aqueveque et al., 2021); flow rate, inclination, vibrating frequency and aperture (Standish et al., 1986). In practice, vibratory screen

* Corresponding author.
E-mail address: kanishk@chalmers.se (K. Bhadani).

https://doi.org/10.1016/j.mineng.2024.108616
Received 11 July 2023; Received in revised form 15 January 2024; Accepted 8 February 2024
Available online 14 February 2024

installation in most production sites is passively controlled, and the performance depends on the initial installation/configuration settings.

To evaluate the process performance of the crushing and screening circuit, multiple key performance indicators (KPIs) such as product or process yield, availability, effectiveness, and overall equipment efficiency (OEE) can be used depending on the objective of plant operation (Bhadani et al., 2020; Gackowiec et al., 2020). To understand and control different KPIs, it is evident that there is a need to estimate the effect of individual equipment variables on the performance of the circuit. In operational research, often a snapshot performance of the process is surveyed (manual physical sampling of material) given a certain condition and scenario (Napier-Munn et al., 1996). In many cases, design variables are varied one factor at a time (OFAT) to get the performance of the unit or a process, given a defined operational range (Bhadani et al., 2021b; Duarte et al., 2021). However, the performance of the circuit can be affected by a combination of unit operational variables (Bhadani et al., 2023). There are instances in the aggregate production field where the effect of multiple variables is studied using the design of experiments (DoE) to evaluate the individual unit operation (Abuhasel, 2022). However, this way of approaching process sampling is limited compared to the modern use of digital data. Parallel with the manual sampling of the circuit, the process is monitored, and key signals are logged to make sure that the process is in stable operation before sampling (Bhadani et al., 2021b). The usage of continuous data is also not utilized to its full potential.

This work aims to apply the systematic framework of design of experiments (DoE) for the operational sampling of an aggregate process to capture information about the process performance. A combination of physical and digital experiments is applied to evaluate performance parameters such as crusher and circuit product yield; screening efficiency; crusher power and power distribution; product shape and quality in a full-scale industrial crushing plant. The framework is also presented on using continuous data to create a process model suitable for optimization applications. Further, the results aim to demonstrate all variables' effects and present interaction effects between the crusher closed-side setting (*CSS*) and eccentric speed (*ES*) on the defined response. Previous experience has shown increased controllability of production using an online control system by varying *CSS* and *ES*, although the quantification of the effects on different products is limited (Hulthén, 2010).

2. Method

The application of DoE is versatile as it is a cost-effective approach to studying a system. From a modelling perspective, DoE can be applied to examine and screen the variables that are having a significant influence on a system output. Then the system output can be modelled based on the variables that have statistical significance. Different sampling techniques can be applied to sample the process, such as full-factorial, fractional factorial, Taguchi and more. This depends on the number of variables involved in the experiment, the process availability, and the purpose of the sampling campaign. (Box et al., 2005; Montgomery and Runger, 2010).

DoE provides a systematic approach to evaluate the variable effect on the output as well as their interaction effect. Doing one factor at a time cannot provide the interaction effect between multiple variables. Each variable (k) is assigned 2 or more levels (l) and then the values of the variables are varied so all different combinations of values are tested together, generating l^k number of experiments. The output is then normalized based on the level of the value for each variable, giving the variables' effect on the output. By plotting the effects in a normal probability plot, variables that have a significant influence on the output can be identified as they deviate from the error line. With each effect, a first-order response can be created to capture the individual effects as well as the interaction effect if there are any for that particular response. In practicality, the selection and combination of variables need to be physically compatible to capture the desired output of interest. (Box et al., 2005; Montgomery and Runger, 2010).

2.1. Applied DoE for crushing plant

The industrial crushing plant used for this study is the tertiary crushing stage in an aggregate quarry. The crushing plant is operated by NCC Industry and is situated in Uddevalla, Sweden. The quarry deposit is a granite rock, and the overall production is over 1 million tons per year, where the process produces up to 20 different products over the year depending on the market request. The tertiary crushing stage is shown in Fig. 1. The process is equipped with a frequency and *CSS*-controlled Metso HP4 crusher which is followed by two consecutive double-deck Metso inclined vibratory screens producing up to six sellable products. The units are interconnected with conveyors which are equipped with power-based mass flow measurements (Bhadani et al., 2021a; Hulthén and Evertsson, 2006). The mass flow units are also connected to cloud-based data storage. The crusher's automatic control for the *CSS* and *ES* was deactivated during the experiments. The mass flow of the fresh feed from the stockpile is regulated by a PI controller.

A DoE was applied to the crushing plant with a full factorial design containing 2 factors and a 3-level approach, where variables *CSS* and *ES* are varied over their operational range, resulting in 9 experiments, see Table 1. The range corresponds to *CSS* = 16, 20 and 24 mm and nominal *ES* +/- 8 %. The eccentric speed was controlled using a variable frequency drive with a nominal value of 50 Hz. The setup for DoE is summarized in Table 1. The selected range of the *CSS* and *ES* was based on the experience of the plant operator and practical limits on the type of crusher to avoid boundary operation conditions. In particular, avoiding the risk of failure of crusher belt-pulley drive (increasing *ES*) and excessive recirculation of material (increasing *CSS*).

The response of the process includes the measured and logged mass flows, the power draw of the crusher, particle size distribution and

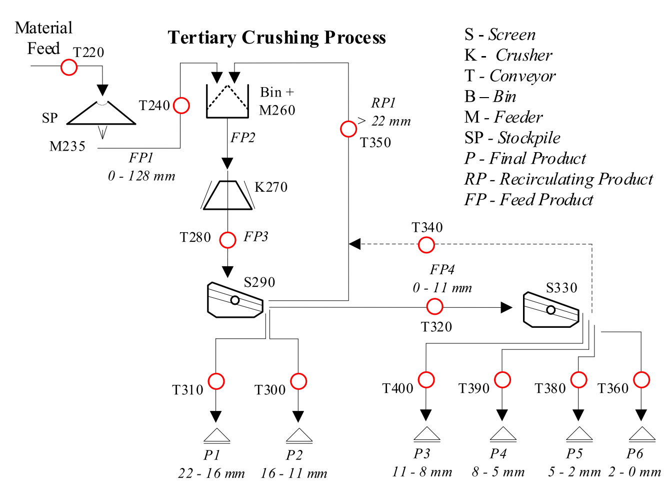

Fig. 1. The tertiary crushing stage of an aggregate plant.

Table 1
Experimental setup for the DOE.

Test Series	CSS	*ES*
X01	CSS1 [-1] 16 mm	Speed1 [-1] − 8 %
X02	CSS1 [-1] 16 mm	Speed2 [0] Nominal
X03	CSS1 [-1] 16 mm	Speed3 [+1] + 8 %
X04	CSS3 [1] 24 mm	Speed1 [-1] − 8 %
X05	CSS3 [1] 24 mm	Speed2 [0] Nominal
X06	CSS3 [1] 24 mm	Speed3 [+1] + 8 %
X07	CSS2 [0] 20 mm	Speed1 [-1] − 8 %
X08	CSS2 [0] 20 mm	Speed2 [0] Nominal
X09	CSS2 [0] 20 mm	Speed3 [+1] + 8 %

flakiness index. A brief process of the experiment is described below and is similar to previous work (Bhadani et al., 2021b).

- The experiment began with the calibration of the crusher *CSS*.
- A series of 9 experiments was performed to get a continuous operation of the crusher at the choke feed condition in steady-state process condition to capture continuous data for mass flow. The process was operated for 15 min to be able to capture the steady-state performance condition. The mass flow at various points on the circuit was logged.
- After 15 min the circuit was crash-stopped to perform the belt-cut sampling at various conveyor points based on the experimental plan.
- For all 9 runs, crusher products were sampled. For two experimental tests (X03 and X04) the entire process was sampled to capture the screens' performance at two loading conditions. For these two particular tests, the screen loading conditions were at an extreme level for the first screen S290. Meaning, that low *CSS* with the high speed of the crusher (X03 - low throughput and more fine material) would produce minimum material throughput on screen S290 and the maximum material yield on screen S330. Comparatively, a high CSS with low speed (X04 - high throughput and more coarse material) would produce maximum material throughput on screen S290 and the minimum material yield on screen S330. The two levels of yield on S330 would potentially produce two throughput levels on S330.
- The belt cut sampling length varied between 0.5 m and 2 m depending on the top size of the material on the belt, uniformity of material distribution and material weight required for sieving analysis. (Napier-Munn et al., 1996; SIS, 2012b).
- For each belt-cut sample, the sieving analysis was performed based on the SS-EN 933–1:2012 standard (SIS, 2012b). For each crusher product belt cut, the flakiness index (FI) was performed based on the SS-EN 933–3:2012 standard (SIS, 2012a).
- The online mass flow data was tested for mass balance consistency while the belt-cut sieve analysis data was checked for known trends in operation.
- The data was post-processed to generate different responses of interest, for example, crusher yield, circuit product yield, etc (Bhadani et al., 2020).
- The experiments were limited in providing evidence and effects for variation in material properties, environmental effects (e.g., moisture) and other uncontrollable variable changes.

For different responses of interests, the DoE model was created. With each effect, a first-order response was created to capture the individual effects as well as the interaction effect if there are any for that particular response. A general form of the generated model is shown in eq. (1)

$$y = \beta_0 + \beta_1 CSS + \beta_2 ES + \beta_3 CSS \cdot ES + \varepsilon \tag{1}$$

where y is the response of the system, *CSS* and *ES* are the two independent variables, β_0 is the intercept, β_1 is the main effect of *CSS*, β_2 is the main effect of *ES*, β_3 is the interaction effect between *CSS* and *ES*, and ε (residual) is the error term in y that is not captured by the model. The response model was fitted using the software JMP Suite Pro 16. The choice of fitting curve to the data can be extended to second or higher-order functions, see Eq. (2), where α_0, α_1, α_2, α_3, α_4, α_5 are fitting parameters for the model and ε (residual) is the error term in y that is not captured by the model.

$$y = \alpha_0 + \alpha_1 CSS + \alpha_2 CSS^2 + \alpha_3 ES + \alpha_4 ES^2 + \alpha_5 CSS \cdot ES + \varepsilon \tag{2}$$

Eq. (3) is used for quantifying the screening efficiency (E), where $\dot{m}_f$ refers to the mass flow rate for the feed material, $\dot{m}_o$ refers to the mass flow rate for the overflow material, f_i refers to the frequency distribution of the PSD for feed material, p_i refers to the frequency distribution of the PSD for overflow material. The index i represents the size interval in the calculation, d is the index of the screening aperture point for the sieve size vector **x**. The formula applied for representing the recovery of the fine material is 100 %, meaning the underflow of the screen does not have coarse material.

$$E = \frac{\dot{m}_f \sum_{i=d}^{n} f_i - \dot{m}_o \sum_{i=d}^{n} p_i}{\dot{m}_f \sum_{i=d}^{n} f_i \left(1 - \dot{m}_o \sum_{i=d}^{n} p_i\right)} \quad where, \tag{3}$$

$$\boldsymbol{x} = [180; 128; 90; 63; 45; 31.5; 22.4; 16; 11.2; 8; 5.6; 4; 2; 1; 0.5; 0.25; 0.125; 0.063]$$

3. Results and analysis

From the 9 experiments, different responses were logged to quantify the system performance. This included the system response in the form of mass flows from all conveyors, particle size distribution from the crusher and other selected sampling points, flakiness of the crusher product and power draw from the crusher. The secondary responses that were calculated include the absolute and relative yield from the crusher product and circuit products, respectively, to get a more detailed view of the system response. The result chapter will be divided into three subsections describing: raw data of experiments; data analysis on product yield between the crusher and the circuit; and data modelling using DoE and effect analysis.

3.1. Raw data of experiments

Fig. 2 provides an overview of the PSD for the crusher feed and product from the experiments in the cumulative and frequency domain. The frequency domain PSD is plotted with the mean size for the sieve size interval. As seen in Fig. 2a, the data confirms the known trend that smaller *CSS* leads to finer crusher products. It can be observed in Fig. 2b, that the peak of the PSD is shifting to finer regions with decreasing CSS. Additionally, for a particular selected CSS, the effect of the speed change is seen in Fig. 2b as the peaks of the PSD shift slightly with increasing the speed of the crusher. This is clearly observed in the frequency PSD in Fig. 2b as compared to the cumulative PSD in Fig. 2a, which shows the difference in the steepness of the curve. This is in line with previously observed trends with speed variation (Hulthén, 2010).

Fig. 3a and 3b provide the particle size distribution for the screening at two different experiments X03 and X04 for the two screens: S290 and S330, respectively. It can be observed that the two-loading condition that was created by two test conditions (X03 – low *CSS* and high speed; and X04 – high *CSS* and low speed) resulted in a differential performance for both screens. Fig. 4 shows the mass flows recorded at different conveyors during the 9 experimental tests. The transient response of the filling up of the crushers can be observed in each test. The data post-processing was used to remove the initial transient state response for modelling purposes. Fig. 5 shows the recorded power draw of the crusher for the 9 experimental tests. Averaging techniques were applied to post-process the continuous data for each test. The experiment X03 was interrupted and continued after a brief stop due to a practical issue.

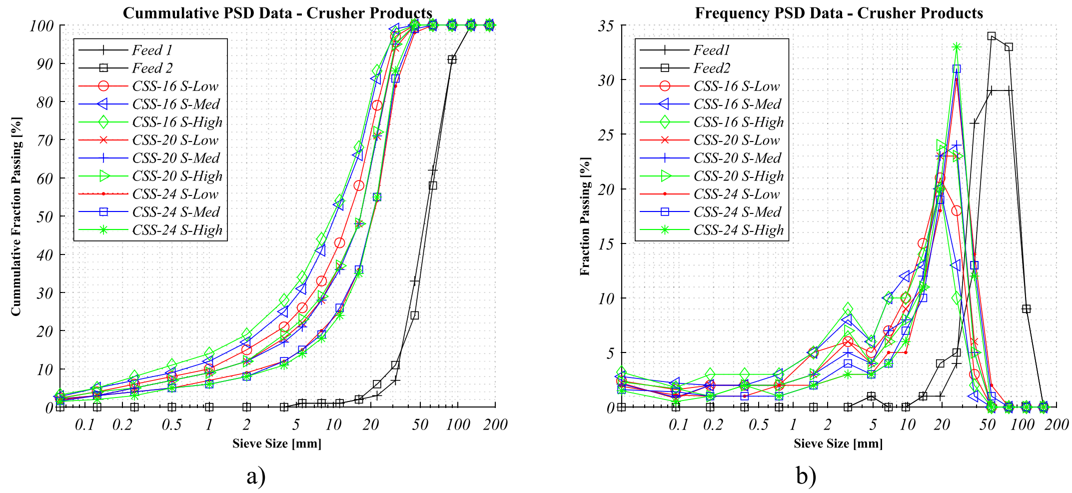

Fig. 2. Particle size distribution for the crusher feed and product from the experiments a) cumulative domain and b) frequency domain.

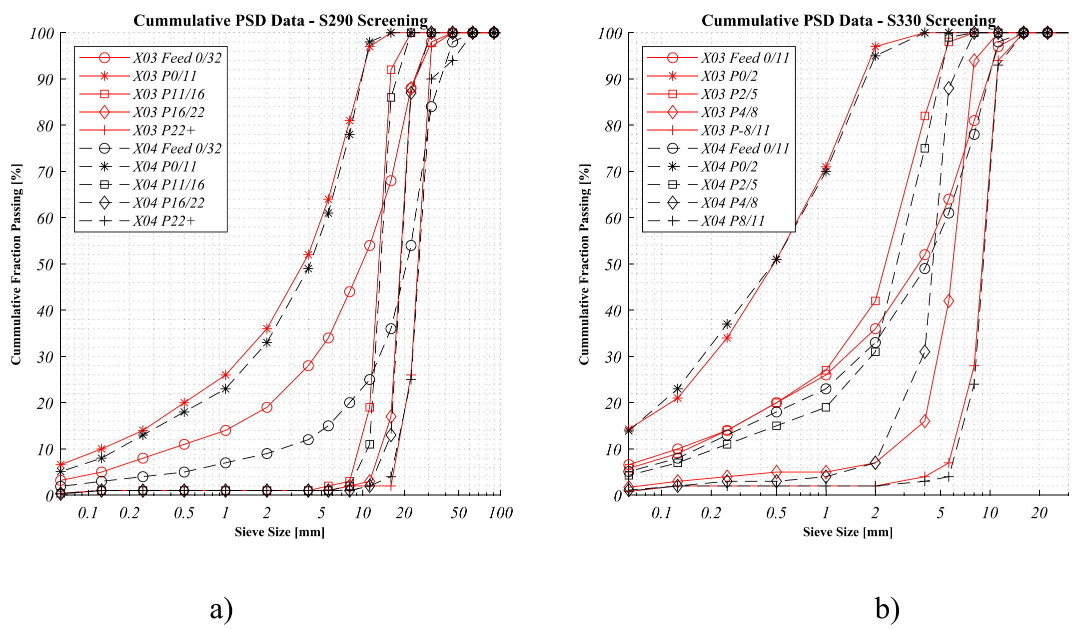

Fig. 3. Particle size distribution for the screening at two different experiments X03 and X04 a) S290 and b) S330.

3.2. Crusher capacity and power modelling

Fig. 6 illustrates a 2nd-order polynomial response model fitted to the crusher capacity from the power-based belt scale as a function of *CSS* and *ES*. Crusher power was monitored to capture both mean values and distribution.

Fig. 7a and 7b illustrate 2nd order polynomial response model fitted to the mean power draw and the standard deviation of the power draw (power distribution) as a function of *CSS* and *ES*, respectively. The power distribution (Fig. 7b) shows a strong correlation with both *CSS* and *ES*, while the correlation between the mean power draw (Fig. 7a) to *ES* is weaker compared to the influence from *CSS*. It can be noted that increasing crusher *ES* lowers variation in power distribution which can be beneficial to the fatigue life of components of the crusher, while the throughput is reduced by around 10 % for the larger CSS (see Fig. 6). The model fitting shows satisfactory error limits for use.

3.3. Data analysis on product yield and quality

As the *CSS* and *ES* change between each run, the particle size distribution from the crusher, as well as the products from the circuit, will change. Table 2 shows the relative yield of each fraction from the crusher and the circuit product. The crusher yield is calculated from the belt cuts from the crusher product while the circuit yield is calculated from the mass flow measurements. Since the objective of the study is to develop methods of simplified models using online data, it is important to understand the implications of using online data on the performance of individual equipment. The mass flow data is a function of the combined performance of the crusher and screen while the process is controlled via the crusher settings and seldom with screen settings.

Table 3 shows the difference between the circuit yield to the crusher yield obtained from data presented in Table 2. These differences are the results of the varying screening performance at different material loading conditions processed at different test settings of the experiment.

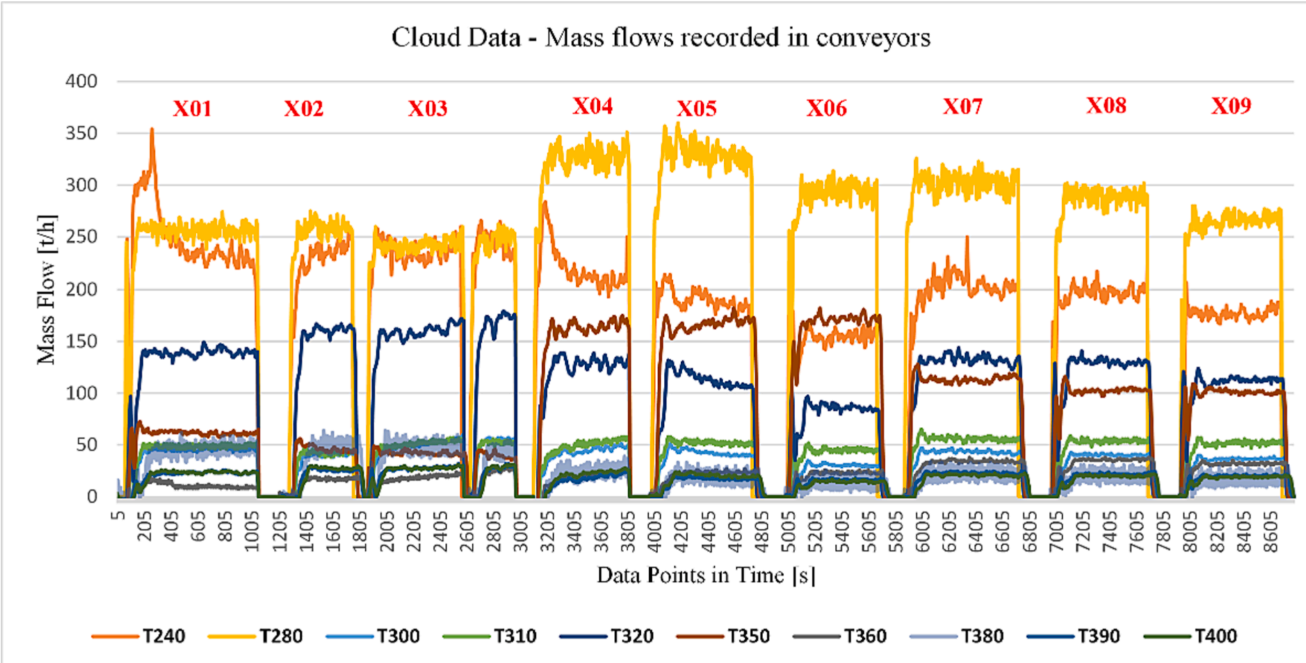

Fig. 4. Mass flow data at different conveyors in the crushing circuit.

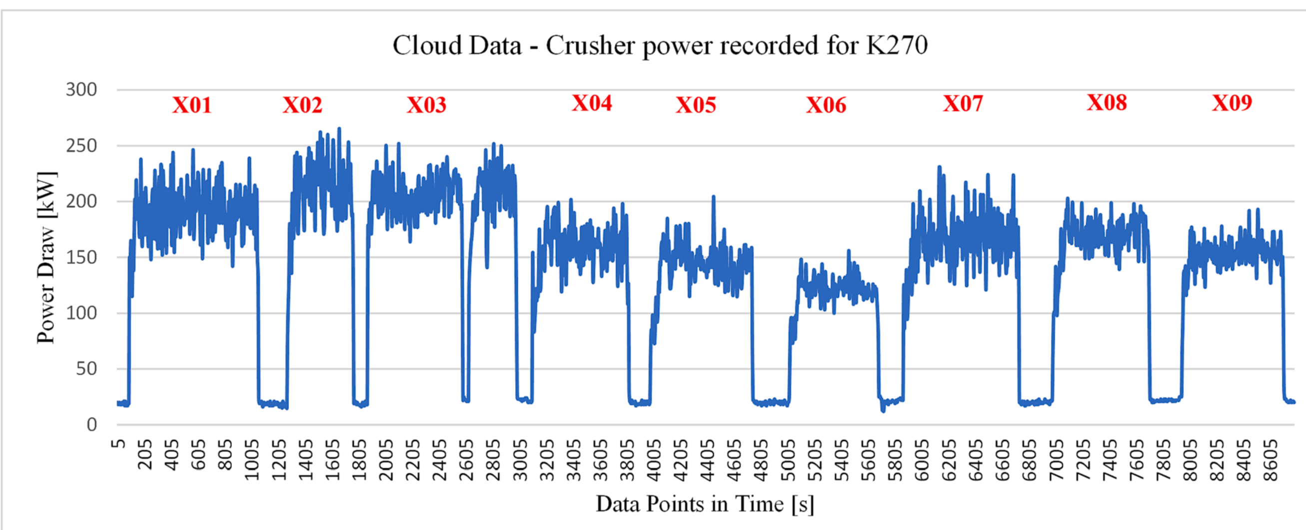

Fig. 5. Recorded power draw of the crusher for the experimental tests.

It can be observed that for the test series X01-X03, the fine products P2/5 and P0/2 show significant deviation compared to other tests. At the smallest *CSS*, the material presented to the screens contained a larger proportion of fine materials compared to coarse material, thus, creating a high load condition for screen S330. After the first 3 experiments at *CSS* = 16 mm, the operator noticed an abnormal flow for the P0/2 mm product. The screen had blinding issues due to a combination of high moisture content in the stream and loading conditions. The screen deck was cleaned, and the experiments continued. From the comparison between the yield from the belt cuts and mass flow from the circuit, there is a clear deviation between the circuit and crusher yield. In contrast, the test series X06 - X09 showed a larger deviation in P + 22 and P16/22 products compared to other tests. Here, the throughput of the crusher was at higher levels due to the open operational *CSS*, resulting in higher loading conditions for screen S290. It is interesting to note that the deviation in X04-X05 showed a lower value for P + 22 despite having higher throughput. This indicates that the screening performance is a function of feed PSD composition together with the throughput, although further investigation is needed to draw conclusive reasons. It could also be an indication that the screen becomes over-dimensioned or under-dimensioned for these varying scenarios in the experiment leading to different performances.

To further understand the screening performance behaviour based on loading conditions, the screening product belt cuts obtained for tests X03 and X04 (see Fig. 3) were analysed and compared with the crusher test for the same (see Fig. 2). The comparison between the crusher and

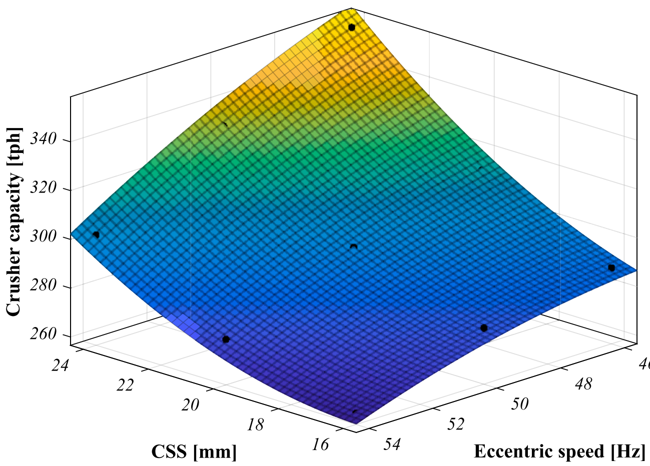

Fig. 6. Crusher capacity modelling using 2nd order polynomial.

screen product yield is shown in Fig. 8 for the two tests X03 and X04. It can be observed that the screening process creates different levels of product yield than the crusher yield because of varying efficiency levels.

Screening efficiency was calculated using Eq. (3) to get an indication of the variability in the screening performance during different operating conditions. In other words, the loading conditions should represent the highest and the lowest loading conditions in the form of throughput. The screening efficiency for screens S290 and S330 for test conditions X03 and X04 is shown in Table 4. It can be concluded that the use of just online mass flow data for modelling comes with limited knowledge of product quality and varying screening efficiency.

Table 3
Absolute difference between the circuit yield to crusher yield of products.

Test Series	+ 22	16/22	11/16	8/11	5/8	2/5	0/2
X01	2.74	−2.13	2.56	−0.84	−0.45	9.44	−11.33
X02	5.02	−2.50	3.43	−1.30	−2.59	7.93	−9.99
X03	4.14	−0.59	4.65	0.33	−2.63	6.31	−12.20
X07	6.73	−4.99	3.31	−2.37	−0.64	−0.89	−1.16
X08	5.69	−4.70	1.71	−1.25	−1.57	0.06	0.05
X09	8.53	−5.38	2.04	−1.23	−0.76	−2.66	−0.54
X04	1.27	−3.11	2.05	1.64	−1.21	2.43	−3.08
X05	3.39	−3.54	2.74	−1.04	−0.44	0.20	−1.31
X06	9.55	−5.55	−1.26	−1.51	−0.38	−0.11	−0.74

Fig. 9 shows the product quality obtained after screening each product for the two tests X03 and X04. Here the quality is represented by the proportion of undersized and oversized particles carried in the product beyond the product specification. There are quality issues observed in the production of P2/5 products as it was also observed in Table 3. Also, for both tests, the first screen S290 has efficiency issues as there are almost 25 % of undersized material is carried over in recirculating product P + 22 for both X03 and X04 tests. This also explains the increased production of P + 22 results in Table 3 for different tests.

From the sampled crusher products, the flakiness was measured to ensure that the quality of the products was not neglected for the sake of higher yield or throughput. Table 5 illustrates the overall flakiness of the different key fractions for the different runs. The flakiness of the coarse product is lower at the CSS operation point which is in line with previous results (Bengtsson and Evertsson, 2006). It is observed that the flakiness of the finer products is lowered by increasing the speed of the crusher,

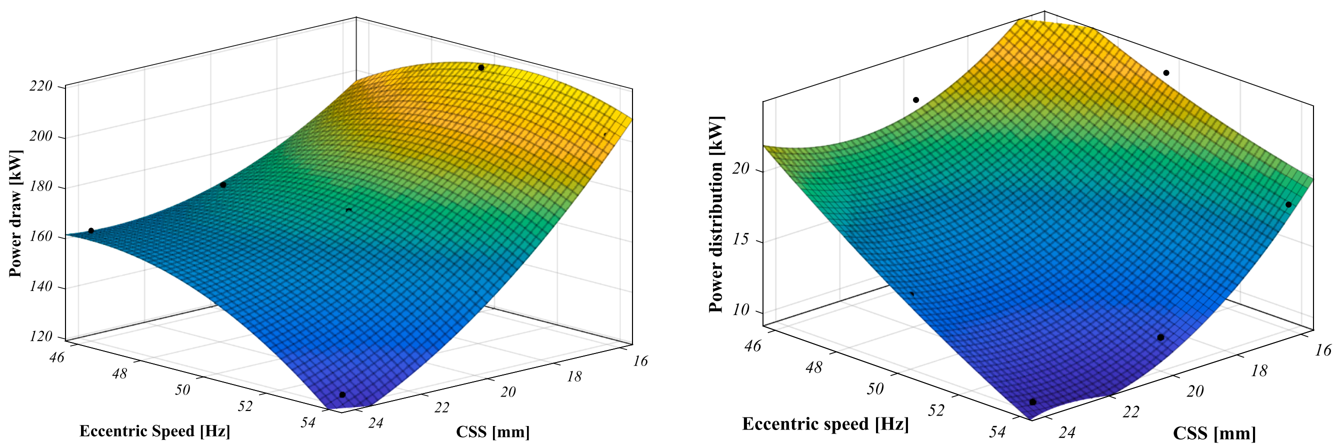

a) b)

Fig. 7. Crusher power modelling: a) fitted model for power, and b) fitted model for power distribution using 2nd order polynomial. Note: the axis of these figures is different from Fig. 6.

Table 2
Yield from the crusher and circuit product for the 9 experimental test conditions.

Test Series	CSS mm	ES Hz	+ 22	16/22	11/16	8/11	5/8	2/5	0/2	+ 22	16/22	11/16	8/11	5/8	2/5	0/2
–			*Crusher yield*							*Circuit yield*						
X01	16	46	21.0	21.0	15.0	10.0	9.5	8.5	15.0	23.7	18.9	17.6	9.2	9.0	17.9	3.7
X02	16	50	14.0	20.0	13.0	12.0	13.0	11.0	17.0	19.0	17.5	16.4	10.7	10.4	18.9	7.0
X03	16	54	12.0	20.0	14.0	10.0	13.0	12.0	19.0	16.1	19.4	18.6	10.3	10.4	18.3	6.8
X07	20	46	29.0	23.0	11.0	9.0	8.0	8.0	12.0	35.7	18.0	14.3	6.6	7.4	7.1	10.8
X08	20	50	29.0	23.0	12.0	8.0	9.0	7.0	12.0	34.7	18.3	13.7	6.8	7.4	7.1	12.1
X09	20	54	28.0	24.0	11.0	8.0	8.0	9.0	12.0	36.5	18.6	13.0	6.8	7.2	6.3	11.5
X04	24	46	46.0	18.0	11.0	5.0	6.5	4.5	9.0	47.3	14.9	13.1	6.6	5.3	6.9	5.9
X05	24	50	45.0	19.0	10.0	7.0	5.5	5.5	8.0	48.4	15.5	12.7	6.0	5.1	5.7	6.7
X06	24	54	45.0	20.0	11.0	6.0	5.5	4.5	8.0	54.6	14.4	9.7	4.5	5.1	4.4	7.3

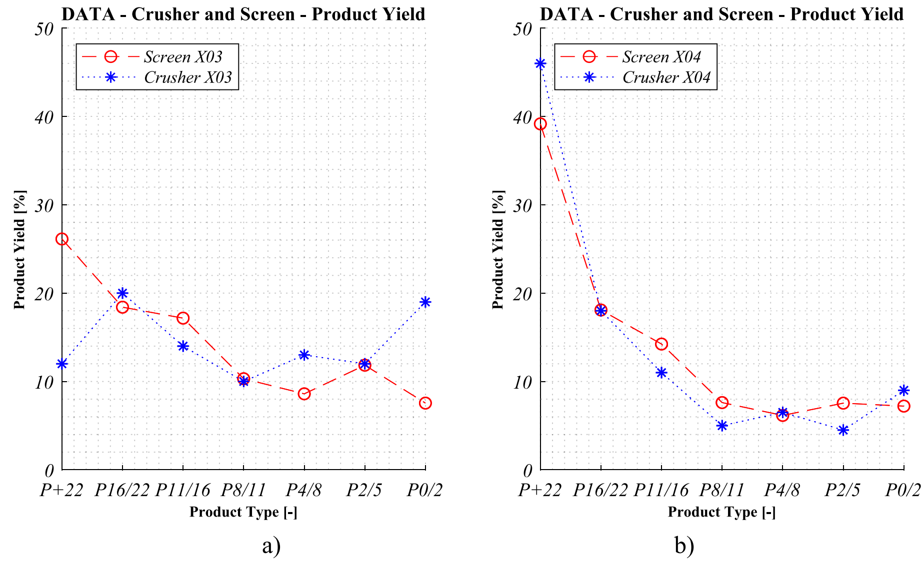

Fig. 8. Comparison of crusher and screen product yield obtained from the belt-cut sampling for a) Test X03 and b) Test X04.

Table 4
Calculated screening efficiency for different screen decks.

S290	Deck 1	Deck 2	Deck 3
X03	0.952	0.948	0.945
X04	0.716	0.930	0.950
S330	**Deck 1**	**Deck 2**	**Deck 3**
X03	0.899	0.833	0.582
X04	0.919	0.702	0.728

especially for lower CSS values (X01-X03). The data indicated both CSS and ES could be used to control the flakiness index of the products, although further investigation is needed to concrete the finding.

3.4. Model fitting using DoE data

By integrating the DoE framework. the effects from different variables can be identified for the different responses. It also opens for an efficient path for black box modelling of individual equipment as well as for the circuit.

Table 6 shows the model fitting parameters and model error using a first-order equation (see Eq. (1) for the different responses captured in the experiments using online data. From an overall perspective, the impact of the *CSS* was ranked with the highest significance on all responses, except the power distribution, where the *ES* had a larger effect. Besides the power distribution, the *ES* was generally ranked second and the interaction effect (*CSS* and *ES*) last, still with a significant effect on few responses. As seen in the model fitting parameters, the magnitude of the effect of each variable varies and the accuracy of the predicted outcome. Most responses fitted well with the first-order equation with an R^2 value of above 0.90 in combination with a lower range of RMSE (root mean square error) values and lower P_{value} showing acceptable confidence in the model. In contrast, the response from y_3 (Crusher Power Distribution) and y_5 (P16/22 Circuit Yield) have lower R^2 values and the response model for y_{11} (P0/2 Circuit Yield) is unacceptable with the first-order equation.

Table 7 shows the model fitting parameters and model error using the second-order equation (see Eq. (2) for the different responses captured in the experiments using online data. This was performed to test the improvements in model fitting for the response which did not fit

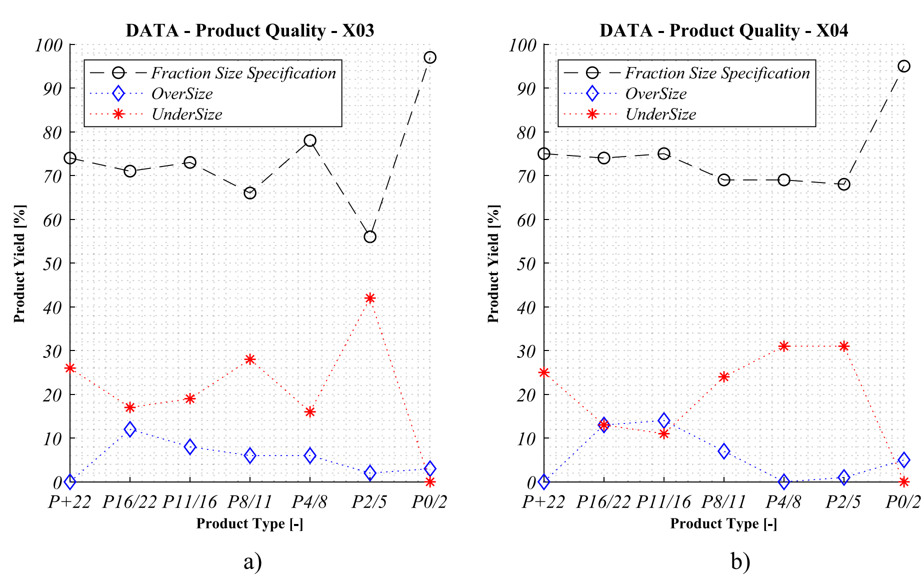

Fig. 9. Comparison of product quality obtained from the belt-cut sampling for the two screens in a) Test X03 and b) Test X04.

Table 5
Crusher product flakiness index based on different bar sizes.

Test Series	CSS	ES	16 mm	12.5 mm	10 mm	8 mm	6.3 mm	5 mm	4 mm	3.15 mm	2.5 mm
X01	16	46	19.9	5.5	2.7	12.6	10.8	9.6	16.7	19.8	28.3
X02	16	50	0	3.5	5.3	5.2	3.8	11.8	16.9	17.3	26.3
X03	16	54	0	0	3.7	8.2	10.9	9.1	13.4	12.9	21.8
X07	20	46	6.7	0	9.2	5.3	15.0	20.0	17.0	19.0	29.8
X08	20	50	3.6	4.7	2.2	14.0	10.1	20.6	24.0	26.0	29.3
X09	20	54	12.7	3.6	8.8	6.0	6.1	13.9	19.9	25.0	25.7
X04	24	46	0	2.6	2.9	13.3	12.4	14.6	27.2	21.3	21.7
X05	24	50	7.2	2.7	8.9	8.5	10.9	16.2	17.4	20.8	28.5
X06	24	54	0	6.2	8.0	11.5	11.0	17.1	20.1	29.8	27.9

Table 6
Model fitting and model error for different responses fitted to first order equation.

Response	Model Response	Model Fitting Parameters				Model Error		
		β_0	β_1	β_2	β_3	RMSE	RSq	PValue
y_1	Crusher Capacity	299.69	26.18	−19.08	−6.37	5.59	0.98	0.0002
y_2	Crusher Power	170.97	−29.31	−7.74	−12.52	10.54	0.92	0.0039
y_3	Crusher Power Distribution	17.39	−3.52	−4.46	−1.26	2.90	0.83	0.0240
y_4	P + 22 Circuit Yield	35.11	15.25	0.08	3.72	1.24	0.99	0.0001
y_5	P16/22 Circuit Yield	17.27	−1.83	0.10	−0.25	1.19	0.74	0.0622
y_6	P11/16 Circuit Yield	14.34	−2.85	−0.61	−1.10	1.01	0.92	0.0040
y_7	P0/11 Circuit Yield	33.23	−10.51	0.40	−2.37	1.87	0.98	0.0002
y_8	P8/11 Circuit Yield	7.5	−2.18	−0.13	−0.80	0.84	0.90	0.0065
y_9	P5/8 Circuit Yield	7.48	−2.38	0.16	−0.40	0.35	0.98	0.0001
y_{10}	P2/5 Circuit Yield	10.28	−6.35	−0.48	−0.75	3.29	0.82	0.0265
y_{11}	P0/2 Circuit Yield	7.97	0.40	0.87	−0.43	3.41	0.10	0.9075

Table 7
Model fitting and model error for different responses fitted to second order equation.

Response	Model Response	Model Fitting Parameters						Model Error		
		α_0	α_1	α_2	α_3	α_4	α_5	RMSE	RSq	PValue
y_1	Crusher Capacity	296.66	26.18	7.95	−19.08	−3.45	−6.37	1.47	0.99	0.0001
y_2	Crusher Power	171.97	−29.31	10.12	−7.75	−11.63	−12.52	5.183	0.99	0.0044
y_3	Crusher Power Distribution	15.02	−3.52	3.01	−4.46	0.55	−1.26	2.79	0.90	0.0930
y_4	P + 22 Circuit Yield	34.55	15.25	−0.78	0.08	1.61	3.72	0.64	0.99	0.0001
y_5	P16/22 Circuit Yield	18.12	−1.83	−1.53	0.10	0.26	−0.25	0.87	0.92	0.0745
y_6	P11/16 Circuit Yield	13.58	−2.85	1.01	−0.61	0.11	−1.1	1.00	0.95	0.0360
y_7	P0/11 Circuit Yield	33.66	−10.51	1.35	0.40	−2.00	−2.37	1.39	0.99	0.0025
y_8	P8/11 Circuit Yield	7.06	−2.18	1.15	−0.13	−0.50	−0.80	0.36	0.98	0.0042
y_9	P5/8 Circuit Yield	7.48	−2.28	0.2	0.16	−0.23	−0.40	0.38	0.98	0.0047
y_{10}	P2/5 Circuit Yield	7.11	−6.35	5.18	−0.48	−0.41	−0.72	0.26	0.99	0.0001
y_{11}	P0/2 Circuit Yield	12.08	0.40	−5.23	0.86	−0.93	−0.42	0.75	0.97	0.0143

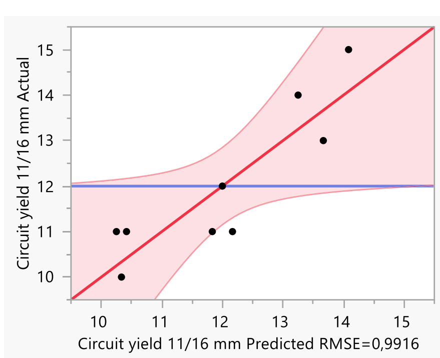

a)

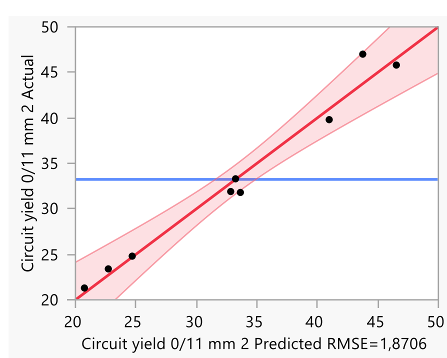

b)

Fig. 10. Model comparison for the circuit yield for the 11/16 mm product and the aggregated yield for 0/11 mm products.

well with first-order equations. The experiment is designed with three levels for each variable which can essentially allow for second-order model fit. As observed with the values in the table, all response model RMSE and R^2 values improved. In particular, y_3 (Crusher Power Distribution), y_5 (P16/22 Circuit Yield) and y_{11} (P0/2 Circuit Yield) resulted in decreased RMSE values and higher R^2 values compared to the first-order model fitting. Although the confidence in the model decreased with increased P_{value}. Based on the two sets of model fitting results, it can be concluded that using the first-order model is sufficient for response prediction and optimization of different performance functions, although it is not guaranteed that all models are within acceptable error values. The use of second-order model fitting provided acceptable limits of model error for all responses.

Circuit yield predictability was largely influenced by the size range of the products. Larger size or multiple size classes have an accurate response while few size classes have less predictability as demonstrated in Fig. 10 a) and b) for the circuit yield. For product yield optimization purposes, it could be beneficial to combine the different response functions to get higher confidence in the results and controllability of the product group instead of individual products. However, certain situation does demand optimization of a particular fraction of the product (Bhadani et al., 2023).

4. Discussion and conclusions

The *CSS* and *ES* have significant impacts on all the responses that can be measured from the crusher. Capacity and particle size distribution have been the focus of several papers and its impact is well documented. Other responses such as the actual circuit yield, power draw and power distribution are however often left out of the quantification of the crusher or system performance. The mean power draw and distribution are also affected by both the *CSS* and *ES*, with the power distribution being amplified with smaller *CSS* and slower *ES*. The complications of increased distribution can include uneven wear, shorter mean time to failure and lower utilization, as discussed by Evertsson et al. (2016). Improved power distribution can potentially have significant improvement in the component life of the crusher (Evertsson et al., 2016; Evertsson et al., 2023). With the presented experimental results, it is recommended to use speed control (*ES*) as an active setting for performance control of the crusher together with the *CSS*, especially for application for product fractions in aggregate production.

The modelling approach using online data together with model fitting with first-order or second-order functions is a computationally cheap approach to map the entire process performance as an operator's guide. The use of simply designed digital experiments using DoE is possible to carry out in other applications where multiple crushers operate in parallel for higher throughput circuits. The opportunities and limitations of the digital experimental approach need to be further tested for complex operations.

With continuous monitoring of the crusher setting, power draw and yield based on circuit throughput, certain production issues can be prevented well in advance before they start to have a significant impact on the product quality. From the comparison between the yield from the belt cuts from crushers and mass flow from the circuit, there is a clear deviation. This could have been detected with limits based on crusher performance and mass flow reading if such logic was in place.

The continuous data of mass flow follows a limitation regarding the reliability of the data if not calibrated periodically. From experience, it has been observed that the mass flow data deviates due to the limitation of the sensors used in the mass flow measurements (Bhadani et al., 2021a). It is recommended to check for the calibration of the mass flow sensor and the mass balancing of the continuous circuit throughput to increase the reliability of circuit yield values. If the background data set used for the DoE models is changing due to the process changes, it is recommended to re-run the sequence of digital experiments to re-create or modify the existing model.

For circuit performance crushers and screens are often analyzed separately. The crusher operation will have a secondary effect on the screening performance based on changing loading conditions, feed size distribution, near size fractions and shape, which in turn all have an impact on the screening performance. In aggregate production it is highly relevant since all products need to follow a specific quality standard and the margin of profit is small.

The reliability of the belt cuts standard practice and is sometimes integrated into the quality assurance at different quarries since all aggregate products need to fulfil the requirements set by the *CE* marking from the intended application. However, these procedures are relatively slow, and all decisions based on the output will be retroactive. The utilization of continuous data is still limited. Cloud-based solutions are gradually being established in the aggregate industry, however, there is a focus on the overall equipment effectiveness (OEE) of selected equipment and the processes (Bhadani et al., 2020; Gackowiec et al., 2020). Based on a similar setup as from the DoE, a systematic approach can be programmed to capture a black-box model of the unit or process to provide suggestions for current demand from the market, maintenance, and stocks. These black-box models are well capable of capturing the necessary system response based on the unit conditions, interaction, and material dependency.

CRediT authorship contribution statement

Kanishk Bhadani: Conceptualization, Formal analysis, Investigation, Methodology, Visualization, Writing – original draft. **Gauti Asbjörnsson:** Conceptualization, Investigation, Visualization, Writing – original draft. **Kristoffer Hofling:** Funding acquisition, Investigation, Resources. **Erik Hulthén:** Conceptualization, Funding acquisition, Investigation, Project administration, Writing – review & editing. **Magnus Evertsson:** Supervision, Writing – review & editing.

Declaration of competing interest

The authors declare that they have no known competing financial interests or personal relationships that could have appeared to influence the work reported in this paper.

Data availability

Data will be made available on request.

Acknowledgements

This work has been performed under the project: "Optimering av verkliga processer för bergmaterialproduktion" and supported financially by "Svenska Byggbranschens Utvecklingsfond"—SBUF, Project Number: 13753 (Development Fund of the Swedish Construction Industry). NCC Industry and their personnel in Glimmingen, Uddevalla are gratefully acknowledged for all their support and efforts to make this work possible. Support from Roctim AB and its personnel is gratefully acknowledged. This work has been performed within the Sustainable Production Initiative and the Production Area of Advance at Chalmers; this support is gratefully acknowledged.

References

Abuhasel, K.A., Aggregate Production Optimization in a Stone-Crushing Plant Using the Taguchi Approach. Proceedings of the National Academy of Sciences, India Section A: Physical Sciences, 2022, **92(1)**, 71-76.

Aqueveque, P., Radrigan, L., Morales, A.S., Willenbrinck, E., 2021. Development of a cyber-physical system to monitor early failures detection in vibrating screens. IEEE Access 9, 145866–145885.

Asbjörnsson, G., Erdem, I., Evertsson, M., 2020. Application of the Hilbert transform for diagnostic and control in crushing. Miner. Eng. 147, 106086.

Asbjörnsson, G., 2015. Crushing Plant Dynamics, PhD Thesis, In *Department of Product and Production Development*. Chalmers University of Technology, Gothenburg, Sweden.

Bearman, R.A., Briggs, C.A., 1998. The active use of crushers to control product requirements. Miner. Eng. 11 (9), 849–859.

Bengtsson, M., Evertsson, C.M., 2006. An empirical model for predicting flakiness in cone crushing. Int. J. Miner. Process. 79 (1), 49–60.

Bengtsson, M., 2009. Quality-Driven Production of Aggregates in Crushing Plants, PhD Thesis, In *Department of Product and Production Development*. Chalmers University of Technology, Gothenburg, Sweden.

Bhadani, K., Asbjörnsson, G., Hulthén, E., Evertsson, C.M., 2020. Development and implementation of key performance indicators for aggregate production using dynamic simulation. Miner. Eng. 145, 106065.

Bhadani, K., Asbjörnsson, G., Hulthén, E., Hofling, K., Evertsson, M., 2021a. Application of optimization method for calibration and maintenance of power-based belt scale. Minerals 11 (4), 412.

Bhadani, K., Asbjörnsson, G., Soldinger Almefelt, M., Hulthén, E., Evertsson, M., 2023. Trade-off curves for performance optimization in a crushing plant. Minerals 13 (10), 1242.

Bhadani, K., Asbjörnsson, G., Schnitzer, B., Quist, J., Hansson, C., Hulthén, E., Evertsson, M., 2021b. Applied Calibration and Validation Method of Dynamic Process Simulation for Crushing Plants. *Minerals*, 11(9) https://www.mdpi.com/2075-163X/11/9/921.

Box, G.E., Hunter, J.S., Hunter, W.G., 2005. Statistics for experimenters. In Wiley series in probability and statistics, Wiley Hoboken, NJ.

Duarte, R.A., Yamashita, A.S., da Silva, M.T., Cota, L.P., Euzébio, T.A.M., 2021. Calibration and Validation of a Cone Crusher Model with Industrial Data. Minerals, 11(11).

Evertsson, C.M., 2000. Cone Crusher Performance. Chalmers University of Technology, Gothenburg, Sweden, In Department of Machine and Vehicle Design. PhD Thesis.

Evertsson, M., Quist, J., Bengtsson, M., Hulthén, E., 2016. Monitoring and validation of life time prediction of cone crusher with respect to loading and feeding conditions, In Comminution 16, Cape Town, South Africa.

Evertsson, M., Quist, J., Bilock, A., Jareteg, K., 2023. Influence of feeding condition on crusher performance and fatigue life, In Comminution 23, Cape Town, 17-20 April, South Africa.

Fuerstenau, D.W., Venkataraman, K.S., 1988. The comminution of multicomponent feeds under batch and locked-cycle conditions: Kinetics, simulation and energy distribution. Int. J. Miner. Process. 22 (1), 105–118.

Gackowiec, P., Podobińska-Staniec, M., Brzychczy, E., Kühlbach, C., Özver, T., 2020. Review of key performance indicators for process monitoring in the mining industry. Energies 13 (19), 5169.

Gröndahl, A., Asbjörnsson, G., Hulthén, E., Evertsson, M., 2018. Diagnostics of cone crusher feed segregation using power draw measurements. Miner. Eng. 127, 15–21.

Guldris Leon, L., Hogmalm, K.J., Bengtsson, M., 2020. Understanding mineral liberation during crushing using grade-by-size analysis—a case study of the Penuota Sn-Ta Mineralization, Spain. Minerals 10 (2), 164.

Hulthén, E., 2010. Real-Time Optimization of Cone Crushers. Chalmers University of Technology, Gothenburg, Sweden, In Department of Product and Production Development. PhD Thesis.

Hulthén, E., Evertsson, C.M., 2006. A cost effective conveyor belt scale, in: 11th European Symposium on Comminution, Budapest, Hungary.

Jacobson, D., Janssen, P., Urbinatti, V., 2010. Cavity level's effect on cone crusher performance and production, in: 7th International Mineral Processing Seminar.

Lee, E., 2012. Optimization of compressive crushing. Department of Applied Mechanics. Chalmers University of Technology, Gothenburg, Sweden. PhD Thesis,.

Lindqvist, M., 2005. Wear in Cone Crusher Chambers. Chalmers University of Technology, Gothenburg, Sweden, In Department of Applied Mechanics. PhD Thesis.

Lindqvist, M., Li, H., 2021. A cone crusher model with a coupled energy- and breakage dependency. Miner. Eng. 172, 107147.

Montgomery, D.C., Runger, G.C., 2010. Applied statistics and probability for engineers. John wiley & sons.

Napier-Munn, T.J., Morrell, S., Morrison, R.D., Kojovic, T., *Mineral Comminution Circuits: Their Operation and Optimisation*. 1996, Julius Kruttschnitt Mineral Research Centre, The University of Queensland, Indooroopilly, Qld Australia.

SIS, S.I.o.S., 2012a. Tests for geometrical properties of aggregates - Part 1: Determination of particle shape - Flakiness Index (SS-EN 933-3:2012). Swedish Institute of Standards, Sweden.

SIS, S.I.o.S., 2012b. Tests for geometrical properties of aggregates - Part 1: Determination of particle size distribution - Sieving method (SS-EN 933-1:2012). Swedish Institute of Standards, Sweden.

Soldinger, M., 2002. Screening of crushed rock material. Chalmers University of Technology, Gothenburg, In Machine and Vehicle Systems.

Standish, N., Bharadwaj, A.K., Hariri-Akbari, G., 1986. A study of the effect of operating variables on the efficiency of a vibrating screen. Powder Technol. 48 (2), 161–172.

Wills, B.A., Finch, J., 2015. Wills' mineral processing technology: an introduction to the practical aspects of ore treatment and mineral recovery. Butterworth-Heinemann.